Uptake and Surface Reaction of Methanol by Sulfuric Acid Solutions Investigated by Vibrational Sum Frequency Generation and Raman Spectroscopies

Lisa L. Van Loon and Heather C. Allen*

Department of Chemistry, The Ohio State University, 100 West 18th Avenue, Columbus, Ohio 43210

Received: December 28, 2007; Revised Manuscript Received: June 4, 2008

The uptake of methanol at the air−liquid interface of 0−96.5 wt % sulfuric acid (H_2SO_4) solutions has been observed directly using vibrational sum frequency generation (VSFG) spectroscopy. As the concentration of H_2SO_4 increases, the VSFG spectra reveal a surface reaction between methanol and H_2SO_4 to form methyl hydrogen sulfate. The surface is saturated with the methyl species after 15 min. The uptake of methyl species into the solutions by Raman spectroscopy was also observed and occurred on a much longer time scale. This suggests that uptake of methanol by sulfuric acid solutions is diffusion-limited.

Introduction

Oxygenated compounds dominate the organic species of the upper troposphere with methanol making up half of all oxygenated organic compound emissions.[1,2] Methanol concentrations up to 1100 ppt have been measured in the remote Pacific troposphere[3–5] and in Asian plumes,[6] while tropospheric concentrations in urban regions are much higher (>20 000 pptv).[3] Due to its much longer lifetime than other compounds such as isoprene methanol is transported from the boundary layer (lifetime = 1 week) to the upper troposphere (lifetime = few weeks) and lower stratosphere.[2,7] Plants are the largest single source of methanol emissions to the atmosphere (37−212 Tg/yr)[1,8] with 67% of emissions from plant growth.[1] Recent continental measurements have shown a diurnal cycle for methanol emissions.[9,10] Rural measurements[11] also show a correlation between methanol emissions and temperature with the lowest emissions recorded during the coldest period of the year. Together, these measurements strongly suggest that biogenic emissions are very important.

Tropical regions are found to be a major contributor to global annual biogenic emissions.[12] Biomass burning plumes are estimated to emit 29−35 Tg CH_3OH/year.[13] In plumes over the Mediterranean, methanol attributed to combustion[6] and methanol found in aged plumes may suggest that oxidation of methane is an important atmospheric source of methanol.[14] However, methanol emissions from biomass burning plumes can be highly variable, suggesting that factors other than hydroxyl reaction with methane determine the methanol concentrations in these plumes.[15] Measurements of methanol in North Atlantic marine air[14] indicate that oxidation of volatile organic compounds (VOCs) is likely to contribute to the observed methanol concentrations several days from the point of emission.

The main tropospheric reaction sink for methanol is its reaction with hydroxyl radical.[3] The ocean is also found to be a slight net sink since the marine boundary layer has slightly lower methanol concentrations than the rest of the troposphere.[5,16] However, there are still large discrepancies between the sources and sinks of methanol.[17]

Sulfuric acid (H_2SO_4) is the predominant aerosol component in the free troposphere.[18] Flight measurements in the troposphere found H_2SO_4 concentrations of 10^4-10^7 molecules cm^{-3} in the upper troposphere to the boundary layer.[19] Although atmospheric sulfur is primarily from anthropogenic sources, sulfate aerosols are distributed throughout both polluted and remote areas. Sulfuric acid is formed from oxidation of sulfur dioxide, a fossil fuel combustion product whose global emissions are estimated at (130−180) Tg of S/yr[20] and also from the oxidation of dimethyl sulfide.[21] At the low temperatures found in the upper troposphere, H_2SO_4 can condense onto preexisting aerosols or nucleate with H_2O to form new aerosols.[21–23] It is thought that $H_2SO_4-H_2O$ nucleation could be responsible for some new particle formation in the marine boundary layer.[24] H_2SO_4 is also involved in nucleation in the remote troposphere. At lower altitudes, $H_2SO_4-H_2O$ nucleation may involve other species, including NH_3.[25] Ammonia is the dominant basic species present in the troposphere and is capable of neutralizing these H_2SO_4 aerosols.[26] While studies show that tropospheric aerosols contain a sizable organic fraction,[27] volatile organic compounds are more likely to condense on preexisting particles, not nucleate new particles.[28,29] The organic matter present in tropospheric aerosols is a complex mixture of acidic oxygenated compounds,[27] so the uptake of small oxidized organics such as methanol by sulfate aerosols may be a mechanism for aerosol growth[30] and may affect the properties of atmospheric aerosols.[31]

In this study, the uptake of methanol by H_2SO_4 solutions ranging from 0 to 96.5 wt % is investigated. First the uptake at the air−liquid interface of H_2SO_4 solutions was investigated using vibrational sum frequency generation spectroscopy (VSFG). The diffusion of methanol into sulfuric acid solutions was monitored using Raman spectroscopy. Finally, the detection limit of methyl hydrogen sulfate (MHS) in H_2SO_4 solutions was determined.

Experimental Section

Vibrational Sum Frequency Generation Spectroscopy. VSFG is an interface selective technique. It is a second-order nonlinear optical probe sensitive to environments lacking inversion symmetry. It has been used to study, among others, solid and liquid surfaces with atmospheric relevance.[32–36] VSFG is sensitive to both the number density and the molecular orientation of the molecules at the interface. Thorough treatments of VSFG theory can be found in the literature[37–40] and a brief introduction is given here.

* Corresponding author. E-mail: allen@chemistry.ohio-state.edu.

10.1021/jp712134s CCC: $40.75
Published on Web 08/01/2008

The intensity of the SFG signal, I_{SFG}, is proportional to the absolute square of the macroscopic nonlinear susceptibility, $\chi^{(2)}$, and to the intensity of the infrared and 800 nm incident beams, as shown in eq 1

$$I_{SFG} \propto |\chi^{(2)}|^2 I(\omega_{IR}) I(\omega_{800}) \quad (1)$$

The macroscopic nonlinear susceptibility, $\chi^{(2)}$, is described by a nonresonant term, $\chi^{(2)}_{NR}$, and the sum of the resonant terms, $\chi^{(2)}_{\nu}$, as shown in eq 2

$$|\chi|^2 = |\chi^{(2)}_{NR} + \sum_{\nu} \chi^{(2)}_{\nu}|^2 \quad (2)$$

When the frequency of the incident infrared beam is resonant with a vibrational mode, ν, then the resonant term dominates the nonlinear susceptibility. The resonant susceptibility term, $\chi^{(2)}_{\nu}$, is related to the number density of the surface species and to the molecular hyperpolarizability, β_{ν}, through the orientationally averaged Euler angle transformation, $\langle \mu_{IJK:lmn} \rangle$, between the laboratory coordinates (IJK) and the molecular coordinates (lmn), as shown in eq 3

$$\chi^{(2)}_{\nu} = N \sum_{lmn} \langle \mu_{IJK:lmn} \rangle \beta^{lmn}_{\nu} \quad (3)$$

The molecular hyperpolarizability is proportional to the infrared transition moment, μ, and the Raman polarizability tensor, α, showing that SFG active modes must be both Raman- and IR-active as shown in eq 4

$$\beta^{lmn}_{\nu} = \frac{-\mu^{n}_{\nu 0}(\alpha^{lm}_{\nu 0})}{2\hbar(\omega_{\nu} - \omega_{IR} - i\Gamma_{\nu})} \quad (4)$$

From eq 4, the resonant macroscopic nonlinear susceptibility is shown in eq 5

$$\chi^{(2)}_{\nu} \propto \frac{A_{\nu}}{\omega_{IR} - \omega_{\nu} + i\Gamma_{\nu}} \quad (5)$$

In the above equation, A_{ν} is the strength of the transition moment and ω_{ν} is the frequency of the transition.

From eqs 4 and 5, it becomes clear that only noncentrosymmetric systems, such as the air−liquid interface, will be SFG-active. When the frequency of a vibrational mode, ω_{ν}, is resonant with the infrared frequency, ω_{IR}, the denominator in eq 5 becomes small, and β_{ν}, and therefore $\chi^{(2)}_{\nu}$, will be enhanced. A VSFG spectrum results from the nonlinear response over the frequency range probed.

BBSFG Instrumentation and Experimental Details. Details of the broad bandwidth SFG (BBSFG) system can be found in previous publications.[41,42] Briefly, two 1 kHz repetition rate regenerative amplifiers (Spectra Physics Spitfire, femtosecond and picosecond versions) are utilized. The picosecond amplifier produces a narrow bandwidth (17 cm^{-1}), 2 ps pulse at a wavelength of ~800 nm. The femtosecond amplifier is used to pump an optical parametric amplifier (Spectra-Physics OPA 800F) to produce a broad bandwidth, ~100 fs, infrared pulse. The spectral window of the IR pulse was ~330 cm^{-1} in the C−H stretching region for these experiments. The energy of the 800 nm beam used was 400 μJ, and the IR energy in the C−H stretching region was 1.0 μJ at the sample. The BBSFG experiment was performed in reflection geometry.

The SFG beam is dispersed spectrally in a monochromator (Acton Research, SpectraPro 500i) using a 1200 g/mm diffraction grating blazed at 750 nm. The SFG signal is collected with a charge-coupled device (CCD) detection system (Roper Scientific, LN400EB, 1340 × 400 pixel array, back-illuminated CCD). Spectral resolution was determined to be 8 cm^{-1}.[43] Calibration of the CCD camera was completed using the 435.833 nm line from a fluorescent lamp.

The polarization combination used in this study is ssp (s-SFG, s−800 nm, p-infrared). The polarization of the 800 nm beam is determined by rotation of a zero-order waveplate. The desired IR beam polarization is determined by rotation of a MgF_2 Berek's compensator. A glan polarizer in the SFG detection line selects the SFG polarization.

The ssp-polarized spectra were obtained continuously with a one-minute acquisition time. Thirty spectra were collected for each uptake experiment. A background spectrum was obtained by changing the temporal overlap of the 800 nm and IR beams. The VSFG spectra are normalized against a smoothed (Savitzky-Golay, second order, 11 points) nonresonant VSFG spectrum from a GaAs crystal to remove any structure present in the IR pulse profile. The dips in a polystyrene-GaAs spectrum are used to calibrate the wavenumber position for each set of experiments.

Raman Spectroscopy. Raman spectra were obtained using 150 mW from a 785 nm continuous wave laser (Raman Systems Inc.) The backscattered light is collected by a fiber optic probe (InPhotonics) coupled to the entrance slit of a 500 mm monochromator (Acton Research, SpectraPro 500i), using a 600 groove/mm grating blazed at 1 μm. The entrance slit width was set at 50 μm and the bandpass, limited by the CCD pixel effective slit width, was measured to be 3 cm^{-1}. In the uptake experiments, spectra were collected as the average of three one-minute exposures every ten minutes for several hours with a liquid nitrogen-cooled CCD camera (Roper Scientific, LN400EB, 1340 × 400 pixel array, back-illuminated and deep depletion CCD). The laser shutter is controlled electronically (Princeton Instruments, ST-133 Controller) to only open during collection to prevent sample heating during the experiment. For the protonation experiments, the laser shutter was opened manually and spectra were collected as the average of three one-minute exposures. Calibration of the CCD camera was completed using the 435.833 nm line from a fluorescent lamp. Acquiring a spectrum of crystalline naphthalene and comparing the experimental peak positions with the accepted literature values completed calibration of the wavenumber position for each set of experiments.[44]

FTIR Spectroscopy. A Thermo Nicolet FTIR spectrometer (Avatar 370, Thermo Electron Corporation) was employed to determine the concentration of methanol in the flow experiments. The N_2/CH_3OH mixture flowed at 25 standard cubic centimeters per minute (SCCM) into an open-ended cell placed in the FTIR sample compartment. Spectra were collected with a spectral resolution of 4 cm^{-1} and 200 scans. A background spectrum was taken and subtracted from each sample spectrum. The gas-phase concentration of methanol was determined by FTIR using the absorbance of the ν_{CO}-ss at 1052 cm^{-1} with equation 6.[45]

$$T = \exp[-kc_m l] \quad (6)$$

T is the infrared transmission. The molar naperian absorption coefficient, k (cm^2/mole), is calculated according to equation 7. The concentration of methanol is c_m. The path length, l, was determined to be 22.86 cm.

$$k = \frac{SN_A}{\Delta\nu} \quad (7)$$

The absorption line intensity, S, for methanol is 3.77 × 10^{-20} cm^{-1}/(molecule cm^{-2}) at 1052.16845 cm^{-1}.[46] N_A is 6.022 × 10^{23} $mole^{-1}$, and $\Delta\nu$ is assumed to be 0.1 cm^{-1}.[45] The concentration of methanol, c_m, with an N_2 flow rate of 25 SCCM

was determined to be $(2.2 \pm 0.2) \times 10^{-7}$ mol/cm^3 or $(1.3 \pm 0.1) \times 10^{17}$ molecules/cm^3.

Chemicals. Methanol (HPLC grade, Fisher Scientific), sulfuric acid (redistilled, 96.5 wt %, GFS), ammonium hydrogensulfate (98%, Aldrich), and nitrogen gas (N.F., min. 99% purity) were used as received. Deionized water was obtained from a Millipore Nanopure system (18.1−18.2 MΩ·cm).

The sulfuric acid solutions were prepared by diluting 96.5 wt % sulfuric acid with deionized water. The concentrations used in the Raman uptake experiments were (79.7 ± 0.3) wt %, (61.6 ± 0.1) wt %, and (39.2 ± 0.1) wt %. For the VSFG uptake experiments the H_2SO_4 solution concentrations were (80.5 ± 0.1) wt %, (57.24 ± 0.02) wt %, and (42.2 ± 0.5) wt %. The differences in H_2SO_4 concentrations used in the VSFG versus the Raman experiments are due to inherent variations in solution preparation. The concentrations were determined to ± 0.1 wt % by titration with a standardized sodium hydroxide solution. To prepare the ammonium hydrogen sulfate solution the salt was dissolved in deionized water and filtered twice through a carbon filter (Carbon-Cap 75, Whatman). The concentration (0.78 ± 0.1 M) was determined spectroscopically using the sulfate vibrational mode at 985 cm^{-1}. (This concentration of NH_4HSO_4 solution is equivalent in the amount of sulfate with a 7.4 wt % H_2SO_4 solution.)

Uptake Experiments. In the VSFG uptake experiments, nitrogen is bubbled into methanol at a flow rate of 25 SCCM (Mass Flow Controller 1479A51CS1BM, powered by PRF4000-F2VIN, MKS Instruments). A three-way valve connects the N_2/CH_3OH mixture flow to the experimental cell (made of Teflon) and to an exhaust line. Prior to the start of an experiment, the mixture flows to the exhaust line. The mixture is allowed to flow into the cell for the duration of the experiments. Between VSFG uptake experiments, the N_2 line is connected directly to the cell for 10 min to flush the cell of any gaseous species. In the Raman uptake experiments, the three-way valve is not used, and instead, the N_2/CH_3OH mixture (CH_3OH concentration of $(1.3 \pm 0.1) \times 10^{17}$ molecules/cm^3) is connected directly to the cell. The Raman probe is placed 3.5 mm below the solution surface. Spectra were reproduced several times over a period of 18 months. All experiments were conducted at room temperature (23 ± 2 °C). Final spectra were collected with the cell lid removed because methanol in the vapor phase absorbs some of the IR radiation. Removing the cell lid allowed for final VSFG spectra to be obtained with maximum signal intensity.

Protonation Experiments. To observe the extent of MHS formation as a function of acidity, seven different H_2SO_4 wt % solutions from 47.1 to 68.3 wt % were prepared. To (5.00 ± 0.01) mL of each solution, (1.000 ± 0.005) mL of CH_3OH was added, and the solutions were stirred overnight to ensure complete mixing. The Raman spectra were then obtained.

Results and Discussion

A previous study by the authors investigated the reaction between methanol and 96.6 wt % sulfuric acid (H_2SO_4) to form methyl hydrogen sulfate (MHS).[35] The experiments were performed by obtaining the VSFG or Raman spectrum after complete mixing occurred. Here the formation of MHS or protonated methanol is investigated in lower wt % H_2SO_4 solutions in real time. Previous investigations by others[47,48] of the uptake of CH_3OH by H_2SO_4 solutions were performed using mass spectrometry to monitor changes in the gas-phase methanol concentration. Using VSFG we are able to monitor spectral changes at the air−liquid interface of the sulfuric acid solutions to determine the methanol species (CH_3OH, $CH_3OH_2^+$, or MHS) present at different H_2SO_4 concentrations.

VSFG Experiments. The ssp polarization VSFG spectra of the uptake of methanol at the surface of H_2SO_4 solutions are shown in Figure 1a−d. One-minute spectra were acquired continuously during the surface uptake experiments. Figure 1e compares the final VSFG spectra obtained for each wt % H_2SO_4, solution, the H_2O solution, and the NH_4HSO_4 solution after the N_2/CH_3OH flow was stopped. The VSFG spectrum of CH_3OH on water agrees with the known spectrum.[42] Ammonia is the predominant basic gas found in the troposphere and is capable of neutralizing acidic sulfate aerosols.[26] NH_4HSO_4 is slightly acidic and for this reason, an NH_4HSO_4 solution was used to determine if a reaction between methanol and bisulfate to form MHS will occur. As shown in the reaction sequence below,[49] the solution must be acidic for the formation of methyl sulfate species.

$$H_2SO_4 + H_2O \leftrightarrows HSO_4^- + H_3O^+ \quad \text{(a)}$$

$$HSO_4^- + H_2O \leftrightarrows SO_4^{2-} + H_3O^+ \quad \text{(b)}$$

$$ROH + H_3O^+ \leftrightarrows ROH_2^+ + H_2O \quad \text{(c)}$$

$$HSO_4^- + ROH + H_3O^+ \leftrightarrows ROSO_3H + 2H_2O \quad \text{(d)}$$

$$ROSO_3H + H_2O \leftrightarrows ROSO_3^- + H_3O^+ \quad \text{(e)}$$

$$ROSO_3H + ROH \leftrightarrows (RO)_2SO_2 + H_2O \quad \text{(f)}$$

The VSFG spectra of H_2O and 0.78 M NH_4HSO_4 solution show the presence of CH_3OH at the surface after the uptake experiment. No CH_3OH peaks were observed for the H_2O and 0.78 M NH_4HSO_4 solutions during the flow experiment. This is attributed to CH_3OH in the vapor phase absorbing the IR radiation at the same wavenumbers as the surface CH_3OH. In Figure 1 (a−d), it is observed that peaks attributable to CH_3OH or MHS were first detectable after 4 to 6 min. No further increase in VSFG signal intensity was observed after 14 to 16 min, suggesting that the surface is fully saturated with CH_3OH or MHS molecules. Absorption of the IR radiation by vapor phase CH_3OH makes the spectral intensity weaker in Figure 1a−d than the final VSFG spectra shown in Figure 1e.

There are three vibrational modes observed in the CH region of the aqueous CH_3OH VSFG spectrum in Figure 1e, the ν_{CH_3}-ss at 2843 cm^{-1} and two Fermi resonances (FR) at 2925 and 2953 cm^{-1}, in agreement with previous VSFG studies.[42,50,51] The observed peak positions change with changing H_2SO_4 concentration due to speciation (CH_3OH, $CH_3OH_2^+$, MHS). The peak positions in each H_2SO_4 solution are found in Table 1. For each of the four H_2SO_4 concentrations investigated (Figure 1a−d), no shifts from the initial peak positions are observed during the flow experiments. However, there are differences in peak positions between H_2SO_4 solutions, as is seen in Figure 1a−e. The peak positions shift to higher wavenumber with increasing H_2SO_4 concentration. Again, in aqueous solution the CH_3OH ν_{CH_3}-ss and FR are found at 2843 and 2954 cm^{-1}. These two peaks are centered at the same positions in 0.78 M NH_4HSO_4. This lack of shift in alcohol peak position from H_2O to NH_4HSO_4 has also been observed for butanol and hexanol.[52] In the four H_2SO_4 solutions investigated, the two peaks blueshift from the positions in H_2O. In 42.2 wt % H_2SO_4, the two peaks shift by 3 cm^{-1} each. With increasing wt % H_2SO_4, the peak shift from the initial CH_3OH peak positions increases to 15 and 18 cm^{-1}, respectively, in 96.5 wt % H_2SO_4. These shifts indicate that new methyl species must be present with the more concentrated H_2SO_4 solutions. In our previous investigation, the

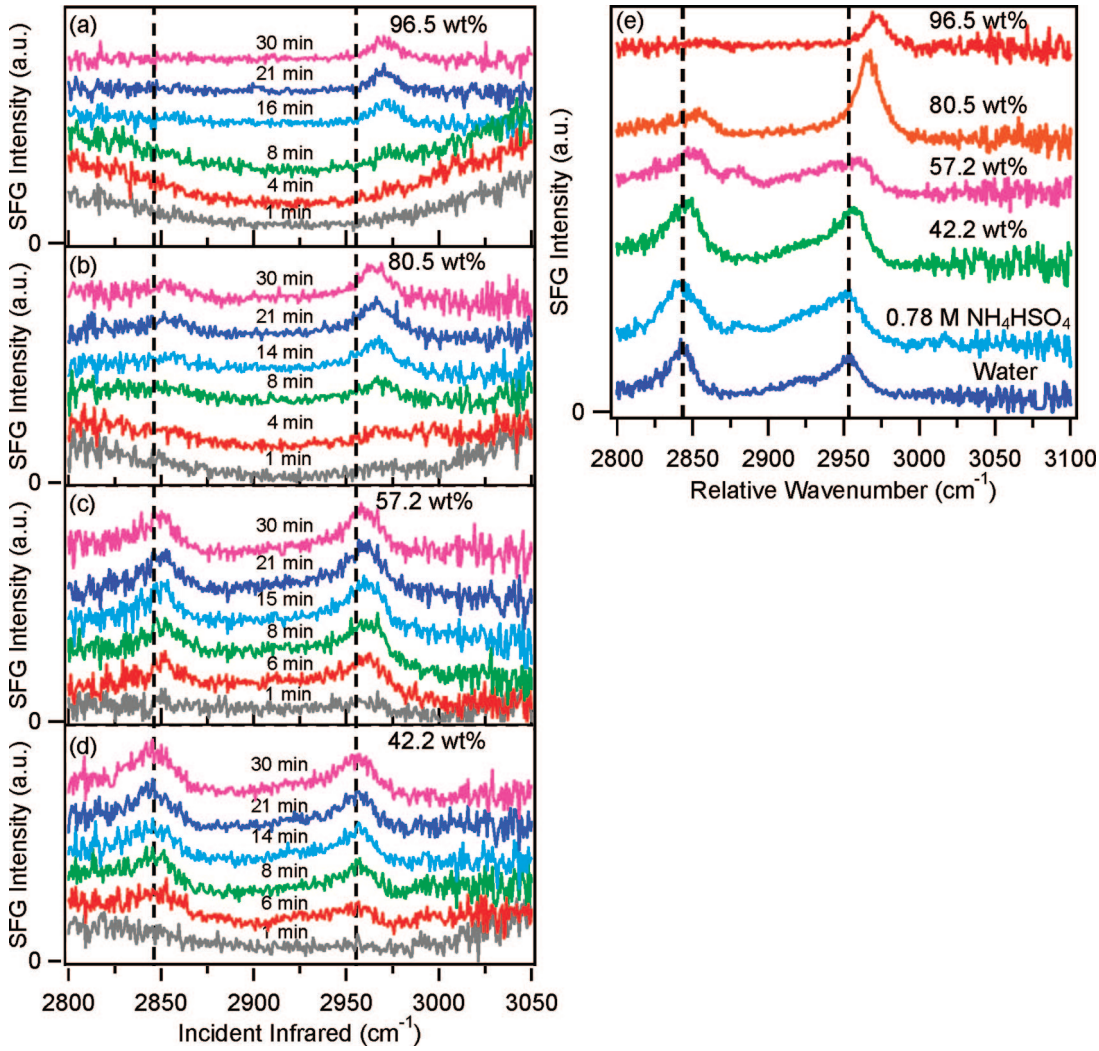

Figure 1. VSFG spectra of the uptake of methanol at the surface of 42.2 to 96.5 wt % H_2SO_4 solutions. (a−d) Methanol was passed over the solution mixtures while VSFG surface spectra were simultaneously being obtained with time. (e) VSFG spectra of the methyl species at the solution air−liquid interfaces after the experiments were completed. Plot e is shown to allow for ease of comparison to plots a−d. The spectra are offset for easier viewing. The dashed lines in a−e are included as guides for the eye for shifts in the position of the CH_3 stretches with changing H_2SO_4 concentration.

TABLE 1: Observed Peak Positions for Two Peaks in the VSFG ssp Spectra and Raman Spectra

VSFG			Raman		
concentration	CH_3OH ν_{CH_3}-ss and MHS FR (cm^{-1})	CH_3OH FR and MHS ν_{CH_3}-ss (cm^{-1})	concentration	CH_3OH ν_{CH_3}-ss and MHS FR (cm^{-1})	CH_3OH FR and MHS ν_{CH_3}-ss (cm^{-1})
96.5 wt %	2858	2972			
80.5 wt %	2854	2967	79.7 wt %	2855	2969
57.2 wt %	2851	2960	61.6 wt %	2856	2961
42.2 wt %	2846	2957	39.2 wt %	2851	2959
0 wt % (water)	2843	2954			
0.78 M NH_4HSO_4	2843	2954			

VSFG spectrum of protonated methanol, $CH_3OH_2^+$, showed a shift in the ν_{CH_3}-ss to 2851 cm^{-1},[35] consistent with the shift observed here from 0 wt % (H_2O) to 42.2 wt % H_2SO_4. In the more concentrated H_2SO_4 solutions, methanol and sulfuric acid are also reacting to form MHS. This is observed as an increase in intensity of the peak observed at 2972 cm^{-1}, attributed to the ν_{CH_3}-ss of MHS.[53] The spectrum in 96.5 wt % H_2SO_4 is in agreement with our previous investigation of the formation of MHS in concentrated H_2SO_4.[35]

Because the peak positions in Figure 1a−d are not changing during each individual flow experiment, the reaction between CH_3OH and H_2SO_4 must be occurring under the spectral acquisition time of 60 s at the air−liquid interface. The first detectable signal occurs in the 4 min spectrum (3−4 min spectrum, 60 s signal accumulation). Using a diffusion coefficient of $(3 \pm 1) \times 10^{-6}$ cm^2/s for methanol into 61.6 wt % H_2SO_4,[54] and knowing the mean square displacement is 2Dt,[55] then the total distance CH_3OH molecules can travel is 0.02 cm into the bulk solution. During this time, it may be possible for a reaction to occur within the top 0.01 cm of the solution, and the reacted species to return to the solution surface. However, if the reaction were occurring on a similar time scale as our signal collection, we would expect to see the initial CH_3OH spectral peaks shift as CH_3OH was protonated by H_2SO_4 to form

$CH_3OH_2^+$ or reacted with H_2SO_4 to form MHS. This is not observed. Therefore, the reaction of CH_3OH must be occurring within the air−H_2SO_4 solution interface. (The air−liquid interface probed in a VSFG experiment is the region where a concentration gradient is found and is not a fixed depth as is understood for a solid surface.)

The relative peak intensities in Figure 1a−d also change with increasing H_2SO_4 concentration. The relative peak intensities are noticeably different for the H_2O, NH_4HSO_4, and 42.2 wt % H_2SO_4 solutions from the more concentrated H_2SO_4 solutions. In the H_2O, NH_4HSO_4, and 42.2 wt % H_2SO_4 solution spectra in Figure 1e, the peaks at 2843 and 2955 cm^{-1} have similar intensities, consistent with the VSFG spectra of CH_3OH in H_2O[50,42,51] and in HCl.[35] In the more concentrated solutions, the peak present at 2970 cm^{-1} is more intense than the one at 2854 cm^{-1} again confirming that the surface methyl species is changed from CH_3OH to $CH_3OH_2^+$ and MHS. This reversal in relative intensities was previously noted for MHS in 96.5 wt % H_2SO_4.[35]

Raman Experiments. The complementary flow experiments monitoring the uptake of methanol or MHS into the H_2SO_4 solutions were performed using Raman spectroscopy. The Raman spectra were collected as one-minute acquisitions every ten minutes during the uptake experiments. The spectra showing the uptake of CH_3OH into the H_2SO_4 solutions are shown in Figure 2a−e. The uptake of CH_3OH into H_2O was monitored by the appearance of the ν_{CO} at 1020 cm^{-1} (Figure 2b). The appearance of the ν_{OSO}-ss at 790 cm^{-1} was monitored for the appearance of MHS in 96.5 wt % H_2SO_4 (Figure 2a). Because of the overlap of H_2SO_4 peaks with the CH_3OH C−O stretch, the uptake of CH_3OH into 39.2, 61.6, and 79.7 wt % H_2SO_4 was monitored in the CH stretching region (2700−3100 cm^{-1}) where no H_2SO_4 peaks are observed (Figure 2c−e). It is important to note that the peaks appear at much later times in the Raman spectra than in the VSFG experiments. The VSFG experiments were conducted on a time scale of minutes while the Raman experiments were done over several hours. Unlike for the surface uptake experiments, the peak intensities in the bulk solutions continued to increase.

As in the surface uptake experiments, the peak positions in each solvent do not shift with time (Figure 2) suggesting that the methyl species present in each solvent do not appear to change during the course of the experiments. From the VSFG experiments it appears that the reaction is occurring at the interface, and then the surfaces species must diffuse into the bulk. (Details of methanol diffusion experiments are found in a companion paper currently in preparation.)[54] The peak shifts and changes in relative intensities are the same as those observed in the VSFG experiments. This indicates that the species present in each solution are the same at the air−liquid interface and in bulk solution.

Protonation versus Reaction. In order for particles to grow through the uptake of volatile oxygenated compounds such as methanol, the compound must condense on the aerosol and its volatility is then reduced. Figure 1e shows the final air−liquid interface spectra of the solutions studied here. The H_2O and 42.2 wt % H_2SO_4 solution spectra are consistent with the known CH_3OH spectrum,[42] suggesting that MHS is not formed in 42.2 wt % H_2SO_4. For this reason it was of interest to determine at what wt % H_2SO_4 concentration, MHS forms and is detected. The Raman spectra of seven different wt % H_2SO_4 solutions to which CH_3OH was initially added and allowed to react are shown in Figure 3a.

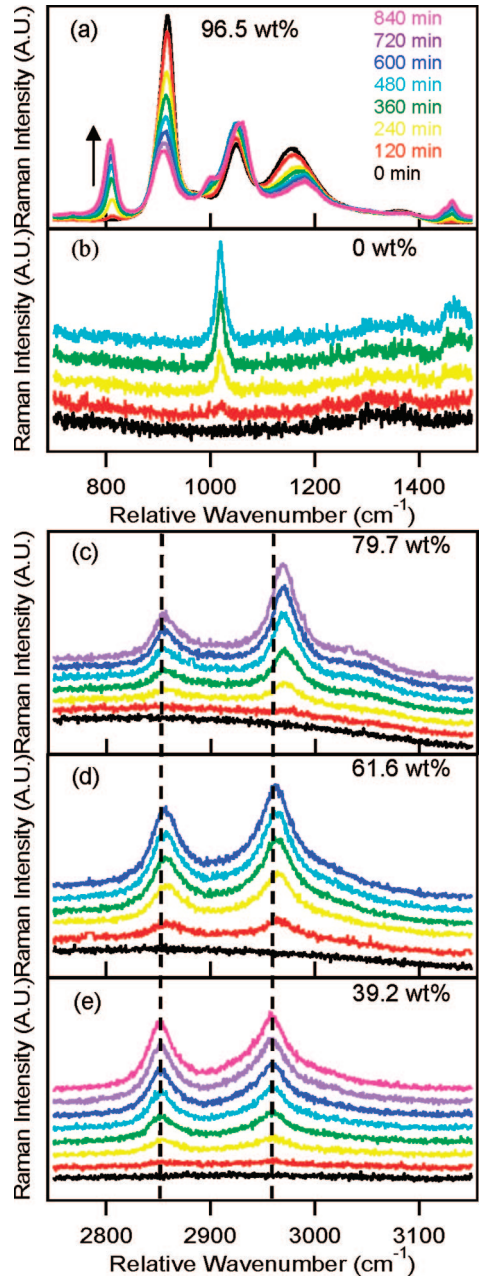

Figure 2. Raman spectra of the uptake of methanol into sulfuric acid solutions. Methanol was passed over the solution mixtures while Raman bulk spectra were simultaneously being obtained. The uptake is observed by (a) the appearance of the ν_{OSO}-ss of MHS at 790 cm^{-1}, (b) the appearance of the ν_{CO} of CH_3OH at 1020 cm^{-1}, and (c−e) the appearance of peaks in the CH_3 stretching region. Panels b−e are offset for easier viewing, where the initial time spectra are shown at the bottom, and the final time spectra are shown at the top.

The expected equilibrium extents of protonation and esterification of methanol in 47.1−68.3 wt % H_2SO_4 were calculated using a pK_{BH+} of −2.05.[56] The expected distributions of CH_3OH, $CH_3OH_2^+$, and MHS are summarized in Table 2. (After the work presented in ref 35 was published, it came to our attention that pK_a's of −4.4 to −4.86[57,58] are much lower than the typical values expected for alcohols. The experiments presented in ref 56 with pK_a's of ∼2 are more accepted. The fact that these two different values for pK_{BH+} have been determined may indicate the difficulty in determining the acidity function in solutions when partial esterification occurs.[59]) To calculate the extent of MHS formation in 47.1−68.3 wt % H_2SO_4 solutions, values for K_{eq} were determined by plotting

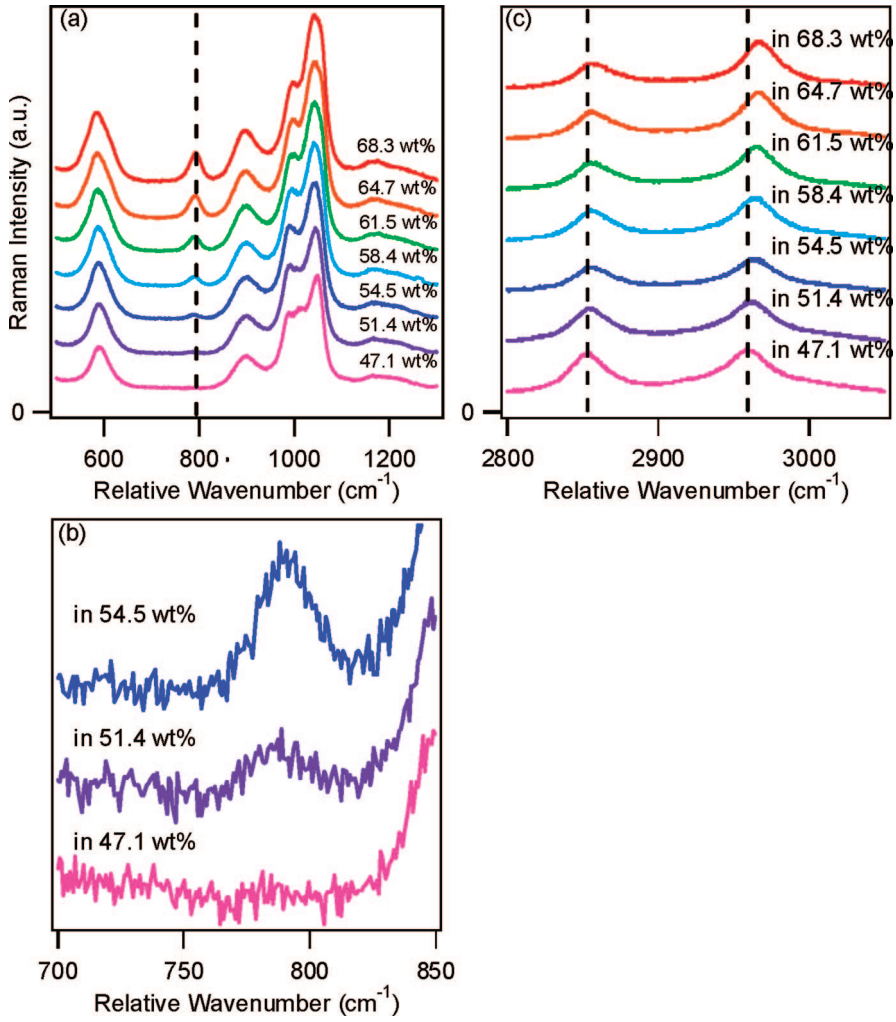

Figure 3. Raman spectra of prepared CH_3OH-H_2SO_4 mixtures (methanol was premixed into the solutions and spectra were then obtained): (a) in the 400−1400 cm^{-1} region, (b) in the 700−850 cm^{-1} region (spectra are enlarged to highlight the appearance of $\nu_{O\text{-}S\text{-}O}$-ss), (c) in the CH stretching region (2800−3050 cm^{-1}).

TABLE 2: The Calculated Equilibrium Distribution of Methyl Species in 47.1−68.3 wt % H_2SO_4 Solutions

wt % H_2SO_4	% CH_3OH	% $CH_3OH_2^+$	% MHS
47.1	76.2	12.4	11.4
51.4	70.8	14.9	14.2
54.5	66.9	17.1	16.0
58.4	62.0	20.3	17.8
61.5	58.1	23.0	19.0
64.7	54.1	26.1	19.8
68.3	49.6	29.9	20.4

the known values of K_{eq}[60] as a function of wt % H_2SO_4. (Further details are presented in the Supporting Information section as well as a comparison of the results using a pK_{BH+} value of −4.86.) In the Raman spectra of the solutions of CH_3OH in 47.1−68.3 wt % H_2SO_4 presented in Figure 3a, the formation of MHS is detected by the appearance of the ν_{OSO}-ss at 790 cm^{-1}. Figure 3b shows the ν_{OSO}-ss region expanded to better determine the first appearance of ν_{OSO}-ss. In 47.1 wt % H_2SO_4, it is calculated that 11.4% of the methyl species is MHS (Table). In 51.4 wt % H_2SO_4, 14.2% of the methyl species is MHS. Since the ν_{OSO}-ss is not easily visible in the 47.1 wt % H_2SO_4 solution, the detection limit of MHS using Raman spectroscopy is determined to be 11−14.2%.

It is also of interest to examine any changes in the CH stretching region that occur with increasing wt % H_2SO_4 and MHS formation (Figure 3c). With increasing wt % H_2SO_4 (and increasing MHS formation), the CH_3OH ν_{CH_3}-ss decreases in intensity. It is possible to compare the changes in peak intensity with the calculated changes in the distributions of CH_3OH, $CH_3OH_2^+$, and MHS with changing wt % H_2SO_4. For example, the decrease in intensity (23%) of the 2850 cm^{-1} peak from the 47.1 wt % solution to the 68.3 wt % H_2SO_4 solution, Figure 3c, is consistent with the observed decrease in the calculated CH_3OH fraction, Table 2. With increasing MHS formation, the peaks in the CH stretching region shift to higher wavenumber (Figure 2c−e) and Figure 3c. The increase in intensity in the peaks observed at 2970 and 3015 cm^{-1} is due to the appearance of the MHS ν_{CH_3}-ss attributed to the increase in MHS concentration with a MHS ν_{CH_3}-ss centered at 2970 cm^{-1}.

These findings suggest that in atmospheric aerosols containing 60+ wt % H_2SO_4, 20% of the methanol that adsorbs to the surface will be transformed into the much less volatile species, MHS. Newly formed, highly acidic aerosols will be expected to experience aerosol growth from the uptake of methanol. As acidic sulfate aerosols in the troposphere age and water and ammonia condense onto them, reducing the acidity, less conversion to MHS will occur.

Conclusions

In this study, the uptake of methanol, both at the surface of and into water and sulfuric acid solutions, was observed directly

using VSFG and Raman spectroscopies. The surface VSFG spectra remain unchanged on the time scale of the uptake experiments. Contributions from methanol, protonated methanol, and methyl hydrogen sulfate (CH_3OH, $CH_3OH_2^+$, and MHS) are observed at the intermediate sulfuric acid concentrations at the surface and in the bulk. Uptake of methanol by sulfuric acid solutions is limited by diffusion of the methyl species into the solutions. Spectral surface-saturation by methanol is observed, while saturation in the bulk solutions is not. This indicates that the liquid surface reaches a steady-state condition with respect to methanol adsorption to the surface. For high sulfuric acid concentrations, the reaction between methanol and sulfuric acid takes place at the air−liquid interface. These results indicate that volatile organic compounds are able to condense onto aqueous H_2SO_4 surfaces to form less volatile species that then can contribute to aerosol growth.

Abbreviations Used

Chemical abbreviations used in this paper are MHS (methyl hydrogen sulfate), which refers to both protonated (CH_3OSO_3H) and unprotonated ($CH_3OSO_3^-$) methyl sulfate. In addition, vibrational sum frequency generation (VSFG), broad bandwidth SFG (BBSFG), symmetric stretch (ss), asymmetric stretch (as), and Fermi resonance (FR) are used.

Acknowledgment. The authors greatly acknowledge the National Science Foundation for financial support (NSF-CAREER CHE-0134131). The authors thank the reviewers for their valuable suggestions.

Supporting Information Available: Details of the equilibrium calculations to determine the distribution of CH_3OH, $CH_3OH_2^+$, and MHS for different wt % H_2SO_4 solutions including plots of H_{ROH} and K_{eq} versus wt % H_2SO_4. Methyl species distributions using a $pK_{BH^+} = -4.86$ and percent conversion values of ethanol to ethyl sulfate.[61] This material is available free of charge via the Internet at http://pubs.acs.org.

References and Notes

(1) Galbally, I. E.; Kirstine, W. *J. Atmos. Chem.* **2002**, *43*, 195–229.
(2) Tie, X.; Guenther, A.; Holland, E. *Geophys. Res. Lett.* **2003**, *30*, ASC 3, doi:10.1029/2003GL017167.
(3) Heikes, B. G.; Chang, W.; Pilson, M. E. Q.; Swift, E.; Singh, H. B.; Guenther, A.; Jacob, D. J.; Field, B. D.; Fall, R.; Riemer, D.; Brand, L. *Global Biogeochem. Cycles* **2002**, *16*, 80, doi:10.1029/2002GB001895.
(4) Singh, H.; Chen, Y.; Staudt, A.; Jacob, D.; Blake, D.; Heikes, B.; Snow, J. *Nature* **2001**, *410*, 1078–1081.
(5) Singh, H. B.; Salas, L. J.; Chatfield, R. B.; Czech, E.; Fried, A.; Walega, J.; Evans, M. J.; Field, B. D.; Jacob, D. J.; Blake, D.; Heikes, B.; Talbot, R.; Sachse, G.; Crawford, J. H.; Avery, M. A.; Sandholm, S.; Fuelberg, H. *J. Geophys. Res.* **2004**, *109*, D15S07. doi:10.1029/2003JD003883.
(6) Scheeren, H. A.; Lelieveld, J.; Roelofs, G. J.; Williams, J.; Fischer, H.; de Reus, M.; de Gouw, J. A.; Warneke, C.; Holzinger, R.; Schlager, H.; Klupfel, T.; Bolder, M.; van der Veen, C.; Lawrence, M. *Atmos. Chem. Phys.* **2003**, *3*, 1589–1608.
(7) Fischer, H.; de Reus, M.; Traub, M.; Williams, J.; Lelieveld, J.; de Gouw, J.; Warneke, C.; Schlager, H.; Minikin, A.; Scheele, R.; Siegmund, P. *Atmos. Chem. Phys.* **2003**, *3*, 739–745.
(8) Fall, R. *Chem. Rev.* **2003**, *103*, 4941–4951.
(9) Karl, T.; Potosnak, M.; Guenther, A. *J. Geophys. Res.* **2004**, *109*, D18306, doi:10.1029/2004JD004738.
(10) Mao, H.; Talbot, R.; Nielsen, C.; Sive, B. *Geophys. Res. Lett.* **2006**, *33*, L02803, doi:10.1029/2005GL024810.
(11) Schade, G. W.; Goldstein, A. H. *Global Biogeochem. Cycles* **2006**, *20*, GB1011, doi:10.1029/2005GB002566.
(12) Lathiere, J.; Hauglustaine, D. A.; Friend, A. D.; De Noblet-Ducoudre, N.; Viovy, N.; Folberth, G. A. *Atmos. Chem. Phys* **2006**, *6*, 2129–2146.
(13) Holzinger, R.; Williams, J.; Salisbury, G.; Klüpfel, T.; de Reus, M.; Traub, M.; Crutzen, P.; Lelieveld, J. *Atmos. Chem. Phys* **2005**, *5*, 39–46.
(14) Lewis, A. C.; Hopkins, J. R.; Carpenter, L. J.; Stanton, J.; Read, K. A.; Pilling, M. J. *Atmos. Chem. Phys.* **2005**, *5*, 1963–1974.
(15) de Gouw, J A.; Warneke, C.; Stohl, A.; Wollny, A. G.; Brock, C. A.; Cooper, O. R.; Holloway, J. S.; Trainer, M.; Fehsenfeld, F. C.; Atlas, E. L.; Donnelly, S. G.; Stroud, V.; Lueb, A. *J. Geophys. Res.* **2006**, *111*, D10303, doi:10.1029/2005JD006175.
(16) Singh, H. B.; Tabazadeh, A.; Evans, M. J.; Field, B. D.; Jacob, D. J.; Sachse, G.; Crawford, J. H.; Shetter, R.; Brune, W. H. *Geophys. Res. Lett.* **2003**, *30*, ASC 13, doi:10.1029/2003GL017933.
(17) Jacob, D. J.; Field, B. D.; Li, Q.; Blake, D. R.; de Gouw, J.; Warneke, C.; Hansel, A.; Wisthaler, A.; Singh, H. B.; Guenther, A. *J. Geophys. Res.* **2005**, *110*, D08303, doi:10.1029/2004JD005172.
(18) Curtius, J.; Sierau, B.; Arnold, F.; de Reus, M.; Strom, J.; Scheeren, H. A.; Lelieveld, J. *J. Geophys. Res.* **2001**, *106*, 31975–31990.
(19) Andronache, C.; Chameides, W. L.; Davis, D. D.; Anderson, B. E.; Pueschel, R. F.; Bandy, A. R.; Thornton, D. C.; Talbot, R. W.; Kasibhatla, P.; Kiang, C. S. *J. Geophys. Res.* **1997**, *102*, 28511–28536.
(20) Brandt, C.; van Eldik, R. *Chem. Rev.* **1995**, *95*, 119–190.
(21) Lucas, D. D.; Prinn, R. G. *Geophys. Res. Lett.* **2003**, *30*, 2136.
(22) Laaksonen, A.; Pirjola, L.; Kulmala, M.; Wohlfrom, K.-H.; Arnold, F.; Raes, F. *J. Geophys. Res.* **2000**, *105*, 1459–1469.
(23) Notholt, J.; Luo, B. P.; Fueglistaler, S.; Weisenstein, D.; Rex, M.; Lawrence, M. G.; Bingemer, H.; Wohltmann, I.; Corti, T.; Warneke, T.; von Kuhlmann, R.; Peter, T. *Geophys. Res. Lett.* **2005**, *32*, L07810.
(24) Clarke, A. D.; Kapustin, V. N.; Eisele, F. L.; Weber, R. J.; McMurry, P. H. *Geophys. Res. Lett.* **1999**, *26*, 2425–2428.
(25) Weber, R. J.; McMurry, P. H.; Mauldin, R. L.; Tanner, D. J.; Eisele, F. L.; Clarke, A. D.; Ka;ustin, V. N. *Geophys. Res. Lett.* **1999**, *26*, 307–310.
(26) Adams, P. J.; Seinfeld, J. H.; Koch, D. M. *J. Geophys. Res.* **1999**, *104*, 13791–13823.
(27) Facchini, M. C.; Mircea, M.; Fuzzi, S.; Charlson, R. J. *Nature* **1999**, *401*, 257–259.
(28) Marti, J. J.; Weber, R. J.; McMurry, P. H. *J. Geophys. Res.* **1997**, *102*, 6331–6339.
(29) Wehner, B.; Petaja, T.; Boy, M.; Engler, C.; Birmili, W.; Tuch, T.; Wiedensohler, A.; Kulmala, M. *Geophys. Res. Lett.* **2005**, *32*, L17810.
(30) Kerminen, V.-M.; Anttila, T.; Lehtinen, K. E. J.; Kulmala, M. *Aerosol Sci. Technol.* **2004**, *38*, 1001–1008.
(31) Noziere, B.; Esteve, W. *Geophys. Res. Lett.* **2005**, *32*, L03812, doi: 10.1029/2004GL021942.
(32) Johnson, C. M.; Tyrode, E.; Baldelli, S.; Rutland, M. W.; Leygraf, C. *J. Phys. Chem. B* **2005**, *109*, 321–328.
(33) Shultz, M. J.; Baldelli, S.; Schnitzer, C.; Simonelli, D. *J. Phys. Chem. B* **2002**, *106*, 5313–5324.
(34) Tarbuck, T. L.; Richmond, G. L. *J. Am. Chem. Soc.* **2006**, *128*, 3256–3267.
(35) Van Loon, L. L.; Allen, H. C. *J. Phys. Chem. B* **2004**, *108*, 17666–17674.
(36) Voss, L. F.; Hadad, C. M.; Allen, H. C. *J. Phys. Chem. B* **2006**, *110*, 19487–19490.
(37) Lambert, A. G.; Davies, P. B.; Neivandt, D. J. *Appl Spectrosc. Rev.* **2005**, *40*, 103–145.
(38) Moad, A. J.; Simpson, G. J. *J. Phys. Chem. B* **2004**, *108*, 3548–3562.
(39) Shen, Y.-R. *Surf. Sci.* **1994**, *299−300*, 551–562.
(40) Zhuang, X.; Miranda, P. B.; Kim, D.; Shen, Y.-R. *Phys. Rev. B* **1999**, *59*, 12632–12640.
(41) Hommel, E. L.; Allen, H. C. *Anal. Sci.* **2001**, *17*, 137–139.
(42) Ma, G.; Allen, H. C. *J. Phys. Chem. B* **2003**, *107*, 6343–6349.
(43) Ma, G.; Allen, H. C. *Photchem. Photobiol.* **2006**, *82*, 1517–1529.
(44) McCreery, R. L. *Raman Spectroscopy for Chemical Analysis*; John Wiley & Sons: New York, 2000.
(45) Hilton, M.; Lettington, A. H.; Mills, I. M. *Meas. Sci. Technol.* **1995**, *6*, 1236–1241.
(46) Rothman, L. S.; Jacquemart, D.; Barbe, A.; Benner, D. C.; Birk, M.; Brown, L. R.; Carleer, M. R.; Chackerian Jr., C.; Chance, K.; Coudert, L. H.; Dana, V.; Devi, V. M.; Flaud, J.-M.; Gamache, R. R.; Goldman, A.; Hartmann, J.-M.; Jucks, K. W.; Maki, A. G.; Mandin, J.-Y.; Massie, S. T.; Orphal, J.; Perrin, A.; Rinsland, C. P.; Smith, M. A. H.; Tennyson, J.; Tolchenov, R. N.; Toth, R. A.; Auwera, J. V.; Varanasi, P.; Wagner, G. *J. Quant. Spectrosc. Radiat. Transfer* **2005**, *96*, 139–204.
(47) Iraci, L. T.; Essin, A. M.; Golden, D. M. *J. Phys. Chem. A* **2002**, *106*, 4054–4060.
(48) Kane, S. M.; Leu, M.-T. *J. Phys. Chem. A* **2001**, *105*, 1411–1415.
(49) Torn, R. D.; Nathanson, G. M. *J. Phys. Chem. B* **2002**, *106*, 8064.
(50) Chen, H.; Gan, W.; Lu, R.; Guo, Y.; Wang, H.-f. *J. Phys. Chem. B* **2005**, *109*, 8064–8075.
(51) Sung, J.; Park, K.; Kim, D. *J. Phys. Chem. B* **2005**, *109*, 18507–18514.
(52) Van Loon, L. L.; Allen, H. C. *J. Phys. Chem. A* **2007**, *111*, 7338–7346.

(53) Bertoluzza, A.; Fagnano, C.; Morelli, M. A.; Tosi, R. *J. Raman. Spec.* **1987**, *18*, 77–81.
(54) Van Loon, L. L.; Allen, H. C.; Wyslouzil, B. *J. Phys. Chem. A*, submitted for publication, 2008.
(55) Jost, W. *Diffusion in solids, liquids, gases*; Academic Press: New York, 1960.
(56) Perdoncin, G.; Scorrano, G. *J. Am. Chem. Soc.* **1977**, *99*, 6983–6986.
(57) Almstead, N.; Christ, W.; Miller, G.; Reilly-Packard, S.; Vargas, K. *Tetrahedron Lett.* **1987**, *28*, 1627–1628.
(58) Weston Jr, R. E.; Ehrenson, S.; Heinzinger, K. *J. Am. Chem. Soc.* **1967**, *89*, 481–486.
(59) Farcasiu, D.; Ghenciu, A.; Miller, G. *J. Catal.* **1992**, *134*, 118–125.
(60) Deno, N. C.; Newman, M. S. *J. Am. Chem. Soc.* **1950**, *72*, 3852–3856.
(61) Clark, D. J.; Williams, G. *J. Chem. Soc.* **1957**, 4218–4221.

JP712134S